Chapter 6

Toughness Assessment and Fracture Mechanism of Brittle Thin Films Under Nano-Indentation

Kunkun Fu, Youhong Tang and Li Chang

Additional information is available at the end of the chapter

http://dx.doi.org/10.5772/64117

Abstract

The nano-indentation technique is an effective tool for assessing the fracture toughness of brittle thin film. In this chapter, a comprehensive and systematic review of toughness measurement methods and fracture mechanisms in brittle film by indentation are presented. The classic method, the energy method, and the stress-based method are three major approaches for determining fracture toughness using the nano-indentation technique. The limits and application ranges of these methods are discussed in detail. In particular, the stress-based method depends highly on the fracture mechanism of cracking. This chapter also reviews different types of crack patterns induced by nano-indentation, such as radial cracks, ring cracks, picture-frame cracks, spiral cracks, and spalling. The possible mechanisms of the crack patterns are investigated considering the substrate effect, the indenter shape effect, and the load level effect. Understanding the fracture mechanism provides guidance in developing a more accurate stress-based model.

Keywords: fracture toughness, fracture mechanism, brittle thin film, nano-indentation

1. Introduction

Over decades, hard thin film has been extensively utilized as protective layers to minimize detrimental influences of the environment. However, hard film usually has a brittle character, and hence fracture failure often occurs in hard thin film when it is subjected to high stress. In designing a high-performance film, it is of great importance to learn the fracture properties of the coating.

Because of the size limitation, the fracture behavior of brittle thin films cannot be easily determined by the standard linear elastic fracture mechanics tension test or the three-point

bending test. In this case, nano-indentation may be the only effective technique to quantitatively characterize the fracture toughness of the film. Anstis et al. [1] were the first to propose an indentation method to evaluate the fracture toughness of brittle materials by measuring the length of radial cracks. In their approach, the assumption was that radial cracks can develop well without any confinement during loading. This classical method has been successfully applied to some "thick" film/substrate systems where radial cracks are well propagated [2–5]. However, it is invalid for brittle thin films/substrate systems because the substrate effect is not negligible and has an effect on crack propagation. For brittle thin films, the energy method proposed by Li et al. [6] has been widely used in recent years for the measurement of fracture toughness although it suffers from some deficiencies that require further research. Subsequently, a number of studies [7–10] have proposed improvements to this energy method. An alternative approach for assessing the fracture toughness of brittle thin films is to use a stress-based model. The most important prerequisite for a stress-based model is understanding the stress distribution in brittle films. Finite element (FE) analysis [11–13] and simplified analytical solutions [14, 15] are two efficient ways to predict stress distribution under indentation. It is evident that stress distribution depends strongly on the indenter shape and the substrate. Different indenter shapes and substrates can result in various crack patterns. A number of indentation-induced crack patterns have been reported, such as radial cracks [16–18], ring cracks [7, 19, 20], picture-frame cracks [21, 22], spiral cracks [23, 24], and spalling [25, 26]. Understanding the mechanism of the above crack patterns by indentation would greatly support the development of a stress-based model.

This chapter proposes a comprehensive and systematic view of fracture toughness assessment methods and fracture mechanisms for brittle thin films under nano-indentation. First, we present a review of the current indentation methods for characterizing the fracture toughness of brittle films, namely the classical method, energy method, numerical method, and stress-based method. The limits and application range of each method are discussed. Next, we review the observation of crack patterns in brittle thin films/substrates under nano-indentation. The various effects of indenter shape, substrate effects, and load levels on crack formation are discussed to gain an understanding of the fracture mechanism of cracking. The chapter concludes with a summary and a roadmap for future trends.

2. Determination of fracture toughness of brittle thin films using nano-indentation

2.1. Classical method

It is agreed that a Vickers' pyramid indenter may produce a median/radial crack pattern in brittle materials. **Figure 1(a)** shows a schematic representation of the median/radial crack pattern induced by a Vickers indenter. The average length of the radial cracks is c_{m}, and a is the impression length. Lawn et al. [27] reported that the elastic/plastic field in material under indentation can be considered as a residual field in an unloaded solid and an ideal elastic field.

http://dx.doi.org/10.5772/64117

Then the fracture toughness of materials can be obtained by measuring the length of the radial crack and the critical indentation load, P, as follows:

$$K_c = \chi \frac{P}{c_m^{3/2}} \tag{1}$$

where χ is a factor relating to the indenter geometry and material properties of the tested specimen and is expressed in the form of

$$\chi = \xi \left(\frac{E}{H} \right)^{2/5} \tag{2}$$

where E and H are the elastic moduli and hardness of the material, respectively. ξ is a constant depending on the indenter geometry and can be determined by linear fitting of the relation between P and $c_m^{3/2}$. A value of 0.016 ± 0.004 for ξ was reported in [1] by experimentally fitting P and $c_m^{3/2}$ for a great variety of brittle materials.

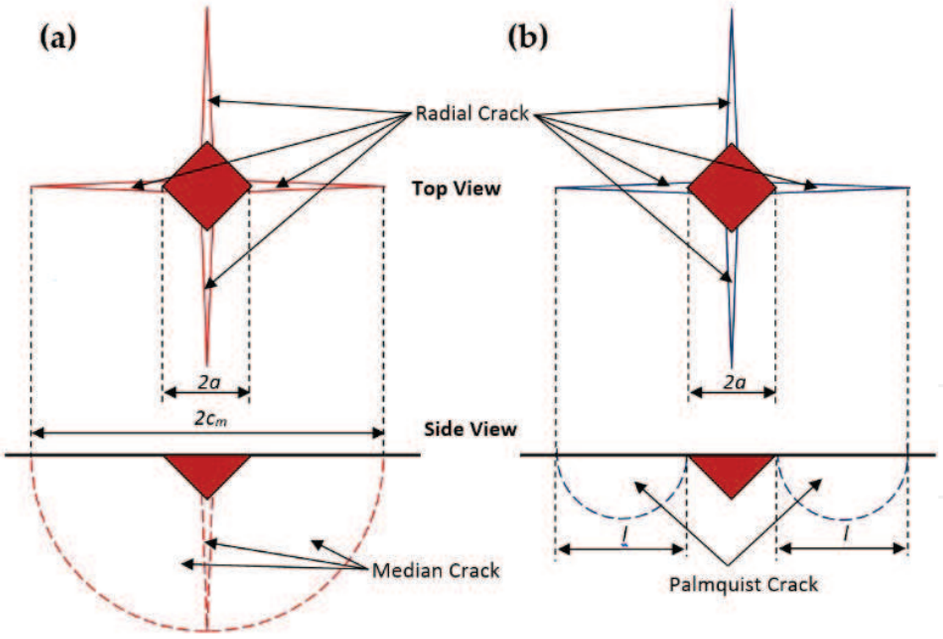

Figure 1. Schematic representation of the crack pattern induced by Vickers indenter: (a) the radial/median crack and (b) the Palmquist crack, based on [28].

The Palmquist crack is another commonly observed crack pattern in brittle materials caused by a Vickers indenter, as shown in **Figure 1(b)**. To assess the fracture toughness of materials in which the Palmquist crack pattern is detected, Eq. (1) needs to be modified as

$$K_c = \xi_v \left(\frac{a}{l}\right)^{1/2} \left(\frac{E}{H}\right)^{2/3} \frac{P}{c_m^{3/2}} \tag{3}$$

where ξ_v is a material constant and has the value of 0.015 reported in [29]. l is the average length of a Palmquist crack.

Although Eqs. (1) and (3) were initially derived from the stress distribution in material under a Vickers indenter, they can be extended to other types of pyramidal indenters, such as a Berkovich indenter and a cube-corner indenter. Comparison of the toughness results of various brittle materials obtained by a Berkovich indenter and a Vickers indenter in [29] showed that the Berkovich indenter could provide more accurate results at a low load range than those of the Vickers indenter, as the shape of the Berkovich indenter is sharper than that of the Vickers indenter. Furthermore, a cube-corner indenter is generally considered the sharpest indenter. It was reported by Pharr [30], therefore, that the cube-corner indenter can significantly reduce the cracking threshold, and is most suitable for toughness measurement of brittle materials at small load compared to other types of pyramidal indenter.

It should be stated that the residual stress in materials has an effect on the elastic/plastic field, and thus on the results of the predicted toughness. If there is a considerable amount of residual stress in brittle materials, Eq. (1) should be changed as follows [31]:

$$K_c = \chi \frac{P}{c_m^{3/2}} + 2m\sigma_R \sqrt{\frac{c_m}{\pi}} \tag{4}$$

where m denotes a dimensionless factor and σ_R denotes the residual stress in the materials.

Eqs. (1)–(4) have been successfully utilized with "thick" film/substrate systems [2–5] where the radial cracks or Palmquist cracks could propagate well. However, the toughness measurement of a "thin" film can be affected by the substrate effect. As a rule of thumb, the substrate effect is negligible when the indentation depth is less than 10% of the film thickness for a soft film/hard substrate. If the film thickness is submicro, the maximum indentation depth should be lower than tens of nanometers in order to minimize the influence of the substrate. However, for most nano-indenters, it is nearly impossible to keep an ideal pyramidal shape on such a small scale. Furthermore, the "1/10 principle" is not adequate for a hard film/soft substrate, which results in an even lower peak depth in order to reduce the influence of the substrate. Therefore, other methods should be employed to evaluate the fracture toughness of brittle thin films.

2.2. Energy method

Theoretically, using the energy method to characterize fracture toughness could minimize the substrate effect. Therefore, the energy method may be the most efficient method for the toughness measurement of brittle thin films. Li et al. [6] were the first to propose an energy

http://dx.doi.org/10.5772/64117

method for assessing the fracture toughness of brittle thin films, and fracture toughness is given by

$$K_c = \left[\left(\frac{E_f}{(1-\nu^2) l_m} \right) \left(\frac{U_{fr}}{t'} \right) \right]^{1/2} \tag{5}$$

where E_f is the film modulus, ν is the Poisson's ratio of the coating, l_m is the crack length in the film plane, U_{fr} is the fracture energy, t' is the effective film thickness, and has the form of

$$t' = t / \sin(\theta) \tag{6}$$

where t is film thickness and θ is the angle of the crack edge.

The key point of the energy method is to identify the dissipated energy according to the indentation load-depth curve. First, the correspondence between the load-depth curve and crack formation needs to be determined. For a perfect "pop-in" as illustrated in **Figure 2(a)**, there is a definite step in the loading curve suggesting where the crack initiates and ends. During the crack formation, a significant amount of energy is dissipated, which causes the discontinuity in the loading curve.

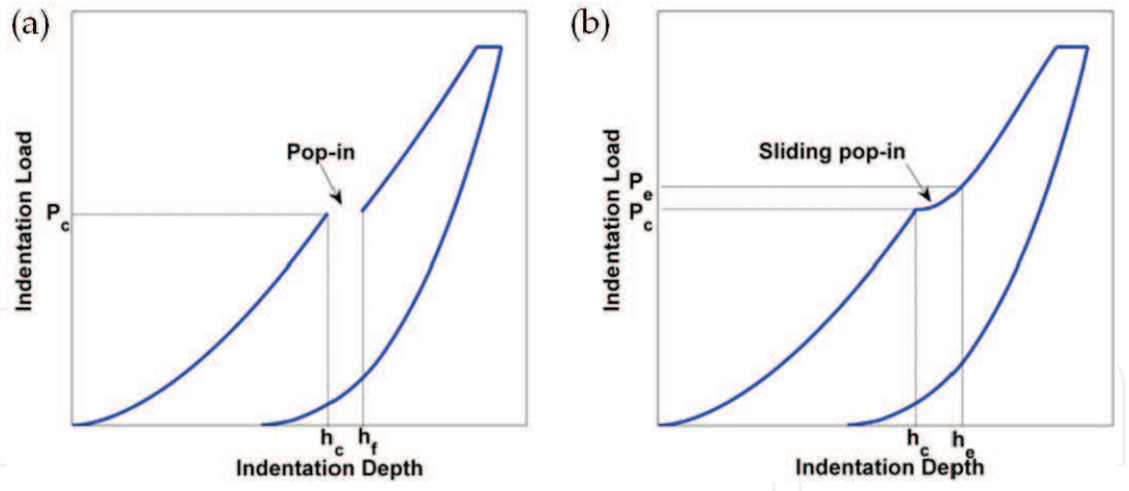

Figure 2. Schematic representation of (a) a perfect "pop-in" and (b) a "sliding pop-in" in load-depth curves [7].

A more general case is a "sliding pop-in" in the load-depth curve when a high-resolution transducer is used in an experiment. In **Figure 2(b)**, there is a clear starting point indicating the crack initiation. However, there is no end point in the load curve. Fu et al. [7] developed a method to define the end point of the "sliding pop-in" in a load-depth curve. They assumed that $\partial P/\partial h^2$ remains constant before and after a circumferential crack formation. **Figure 3** shows $\partial P/\partial h^2$ as a function of h^2. A quick drop of $\partial P/\partial h^2$ is observed, indicating the onset point of the "sliding pop-in" in the load-depth curve and also the initiation of the circumferential crack.

After the crack is complete, the derivative $\partial P/\partial h^2$ becomes stable again and the value is similar to that before the crack initiation. Accordingly, the end point of the "sliding pop-in" is identified.

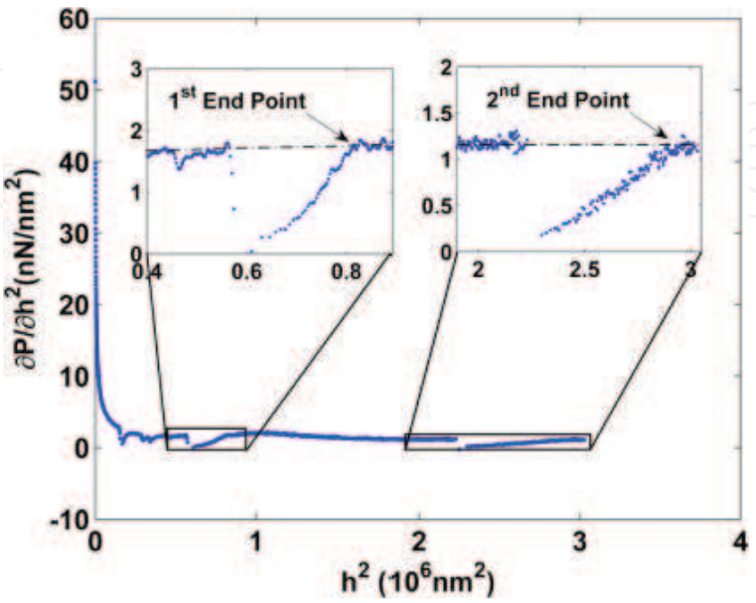

Figure 3. A method to define the end point of a "sliding pop-in" [7].

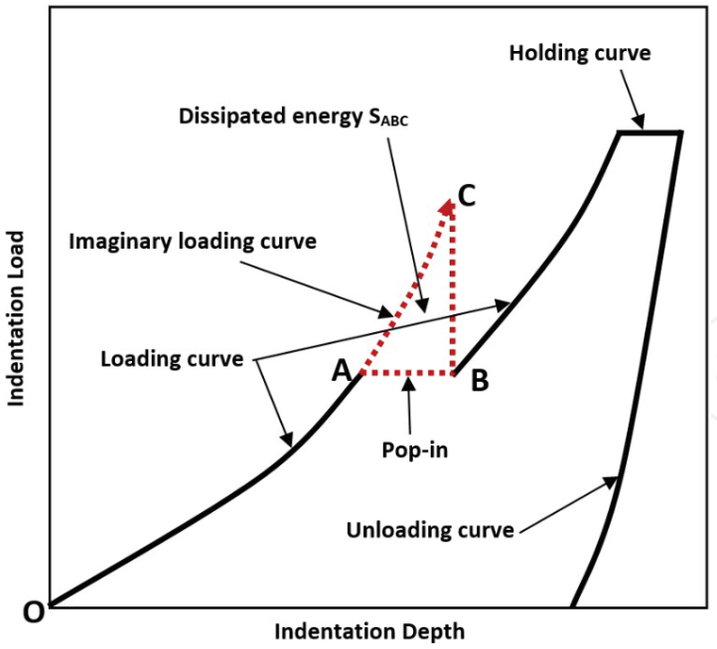

Figure 4. Schematic representation of a method to obtain the dissipated energy.

After the start point and end point of the crack in a loading curve have been obtained, the dissipated energy during crack formation may be calculated by different methods. For

http://dx.doi.org/10.5772/64117

instance, a schematic of the load-depth curve in [6] is illustrated in **Figure 4**. The crack initiates at point A and ends at point B. If the crack does not occur, the loading curve follows the trend of the OA curve and reaches the point C. Hence, the enclosed area S_{ABC} is assumed to represent the dissipated energy during cracking [6]. This method is widely used to evaluate the fracture toughness of thin films, even though it ignores the change in elastic-plastic stress distribution of the film before and after crack propagation.

Given the shortcomings of the method in [6], Chen et al. [8] developed another method to define the dissipated energy by using the curve of total work as a function of displacement. **Figure 5** shows that a crack initiates at A and ends at D. The first work-displacement curve is extrapolated from A to C, and the second work-displacement curve is extrapolated from D to B. The work difference between CD and AB is considered to represent the dissipated energy during the crack formation. The negative or positive of AB relies on the film/substrate system. This method examines the work difference before and after cracking, and thus the energy caused by the change of elastic-plastic behavior is excluded. However, the accuracy of this method is still dependent on extrapolation of the imaginary work-displacement curves.

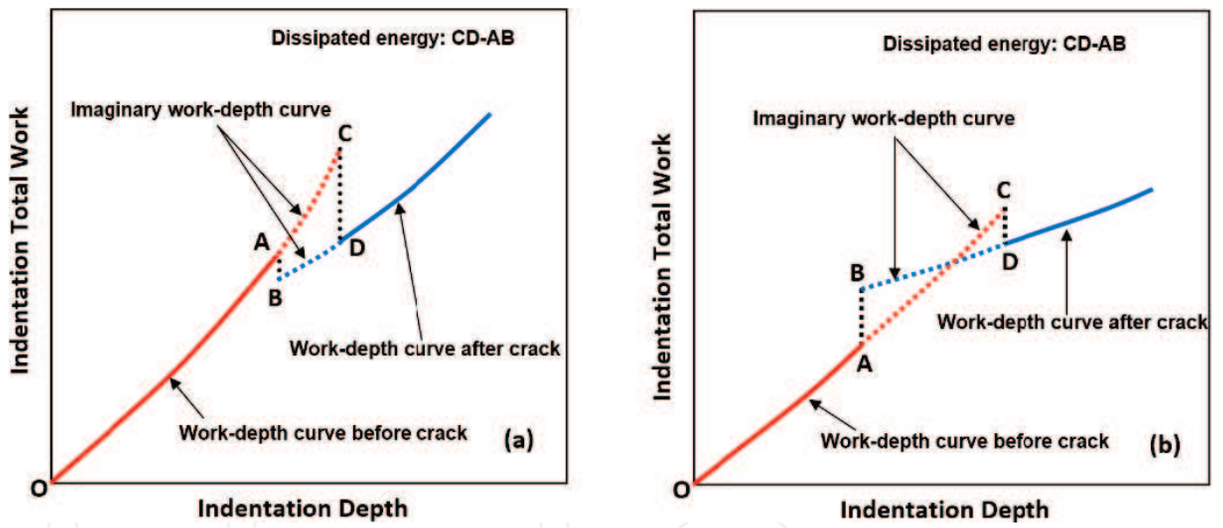

Figure 5. Schematic representation of a method to determine the dissipated energy CD-AB. Compared to CD, AB is positive in (a) or negative in (b), depending on the actual coated systems.

There are also a few studies focusing on estimating the bounds of the fracture energy. For instance, Toonder et al. [9] proposed an approach to evaluate the upper and lower limits of fracture energy by considering a material as pure elastic or perfect plastic. In **Figure 6(a)**, if the film/substrate system behaves as an elastic material, all the deformation will recover after unloading as the dashed curve BO. If the film/substrate system displays perfect plastic behavior, there is no elastic recovery. The unloading curves before and after the crack will be AC and BD, respectively. In practice, the film/substrate system is an elastic-perfect plastic material, and therefore, the dissipated energy should be between the enclosed area of ABO and ABDC. Hence, the upper and lower limits of the dissipated energy during cracking are given by

$$\frac{2}{3}P_{cr}(\delta_2-\delta_1)\le U_{fr}<P_{cr}(\delta_2-\delta_1) \tag{7}$$

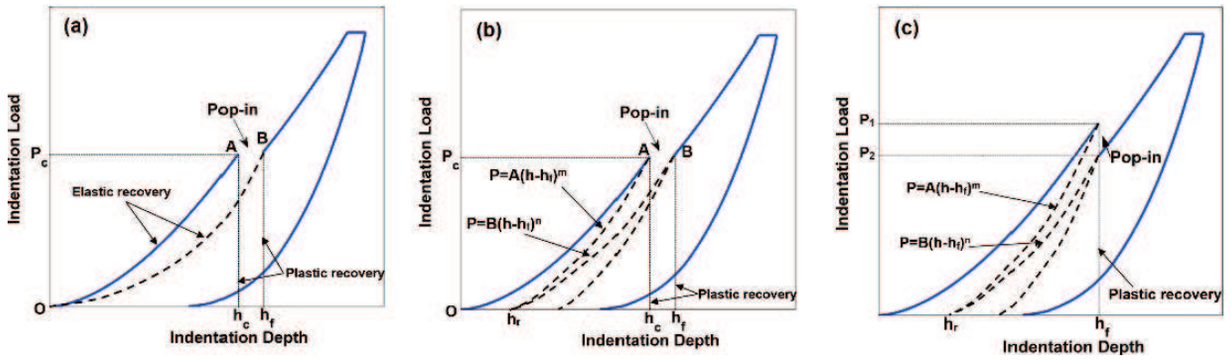

Figure 6. (a) A method and (b) an improved method to define dissipated energy using load control and (c) displacement control.

Further, Chen et al. [10] enhanced the method in [9] by performing a more reliable analysis of the unloading curves, as shown in **Figure 6(b)**. The bounds of the fracture toughness are expressed as

$$\int_{\delta_f}^{\delta_1}A(x-\delta_f)^m\,dx+P_{cr}(\delta_2-\delta_1)\ge U_{fr}>\int_0^{P_{cr}}\left((\frac{y}{B})^{1/n}-(\frac{y}{A})^{1/m}\right)dy \tag{8}$$

Similarly, an approach to calculate the bounds of fracture energy of the film system under a displacement control is shown in **Figure 6(c)**. The dissipated energy is given by [10]

$$\int_{\delta_f}^{\delta_{cr}}A(x-\delta_f)^m\,dx\ge U_{fr}>\int_{\delta_f}^{\delta_{cr}}\left(A(x-\delta_f)^m-B(x-\delta_f)^n\right)dx \tag{9}$$

The energy method is efficient for obtaining the fracture toughness of brittle thin films because there is no need for information about crack propagation, such as crack size. However, the accuracy of the energy method depends highly on either the extrapolated imaginary load-depth curve or the imaginary total work-displacement curve. In experiments, it is impossible to know the accuracy of the imaginary extrapolated curve as the trend of the loading curve can be affected by many factors, such as roughness of the surface, defects in the films and the ratio of indentation depth to film thickness.

2.3. Stress-based method

The stress-based method is a straightforward approach for assessing the fracture toughness of brittle thin films. It is based on stress distribution in the brittle thin film under an indenter. To

http://dx.doi.org/10.5772/64117

date, some analytical solutions have been derived for stress distribution in an incompressible elastic coating [32], compressible elastic coating/rigid substrate [33], and elastic film/elastic substrate [34, 35]. However, due to the complex elastic-plastic properties of film and substrate and the boundary condition of the indenter and film, it is not feasible to derive an analytical solution for evaluating the stress distribution in the brittle film/elastic-plastic substrate system. FE analysis is a useful tool for obtaining the fracture stress in film under indentation. Hence, stress distribution in a film is usually determined using FE analysis. For example, for a brittle film on a ductile substrate, the stress distribution under a conical indenter is obtained by FE analysis and is shown in **Figure 7**. A high tensile radial stress occurs at the surface of a film, which can open a crack.

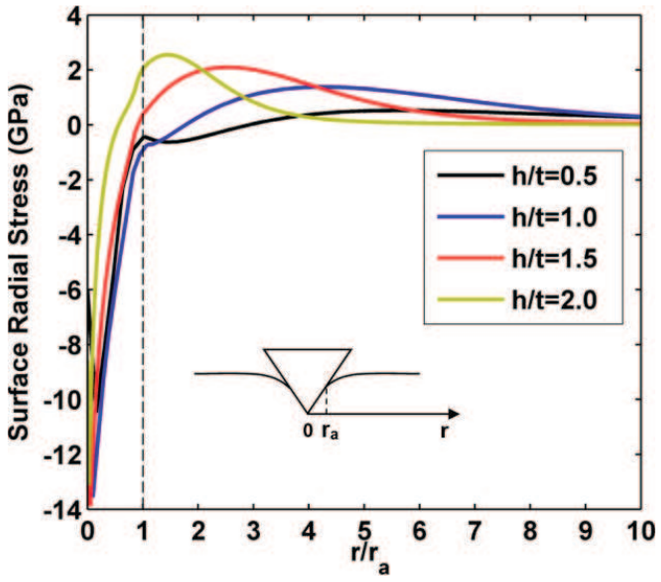

Figure 7. Radial stress in film at the surface for various ratios of indentation depth *h* and film thickness *t* [7].

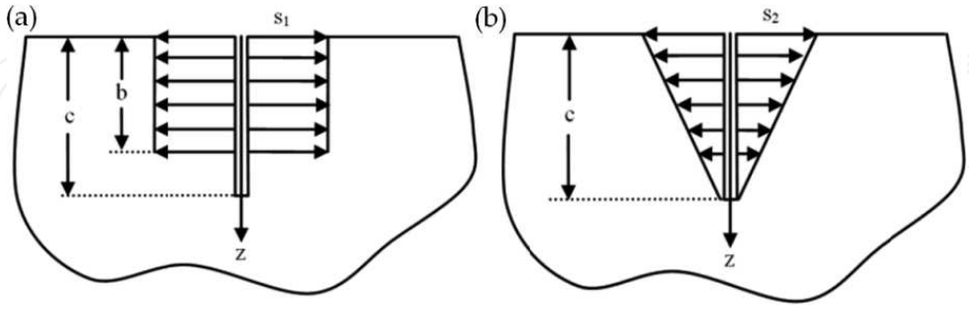

Figure 8. Stress applied to a crack during indentation: (a) constant stress and (b) linear stress [15].

When the stress distribution in a film has been obtained, the fracture toughness can be obtained by assuming the stress on pre-existing cracks as a uniformly distributed crack and a linearly distributed crack as shown in **Figure 8(a)** and **(b)**. Based on the linear fracture mechanics, fracture toughness is expressed as

$$K_{\mathrm{I1}} = 1.12 s_1 \sqrt{\pi c} + 0.439 s_2 \sqrt{\pi c} \tag{10}$$

where s_1 is a constant stress, s_2 is the highest stress in a linear stress distribution, b is the crack length, and 1.12 and 0.439 are the geometric factors in **Figure 8(a)** and **(b)**, respectively.

An initial short crack may grow to a circumferential channel crack by self-adjusting to a curved shape when the energy release rate G_{ps} by linear fracture mechanics is the same at each point, as reported by Steffensen et al. [11]. The energy release rate for the circumferential channel crack, G_{ss}, is given by

$$G_{\mathrm{ss}}(c) = \frac{1}{c}\int_0^c G_{\mathrm{ps}}(\tilde{c})\mathrm{d}\tilde{c} \tag{11}$$

G_{ps} is expressed as

$$G_{\mathrm{ps}} = K_{\mathrm{I}}^2\left(\frac{1-\nu^2}{E_{\mathrm{f}}}\right) \tag{12}$$

Then the fracture toughness can be obtained by calculating the maximum of G_{ss} as proposed by Madsen et al. [12],

$$G_{\mathrm{c}} = \max(G_{\mathrm{ss}}(c)) \tag{13}$$

An alternative method for determining the fracture stress and thus the fracture toughness is to use a simplified stress-based model. The simplified model can give an explicit expression of fracture stress for a particular type of coated system. For example, Morasch and Bahr [14] developed a method to identify stress distribution of a brittle film/ductile substrate under an axisymmetric indenter. In their model, they believed that the ring crack was mainly induced by the film bending. Thus, the indentation load is assumed as a pressure with a radius of a_c, and the plastic zone is considered as a uniform distributed pressure. The bending moment by these two types of pressure is given by

$$M_\theta = \frac{P}{4\pi}(1+\nu)\left(\frac{a_{\mathrm{c}}^2}{4c^2} - \ln\frac{a_{\mathrm{c}}}{c}\right) - \frac{p_0 c^2}{8} \tag{14}$$

Then the bending stress can be obtained as

$$\sigma_{\mathrm{rr}} = \frac{12 M_\theta}{t^3} z \tag{15}$$

http://dx.doi.org/10.5772/64117

where z is the distance from the middle surface of the circular plate. It is clear that the maximum radial stresses occur on the surfaces $z = \pm t/2$ of the plate. This coincides with observations from the literature [7] that circumferential cracks initiate from the top surface of the brittle film. When the radial stress on top of the film surface reaches the strength, circumferential cracks initiate and begin to propagate along the interface between the film and the substrate. **Figure 9** shows the pressure distribution in the coated system with a modulus ratio of 14.0–69.8 under a spherical indenter and a conical indenter by FE analysis; however, it has been found that the pressure caused by the plastic zone is clearly not uniform.

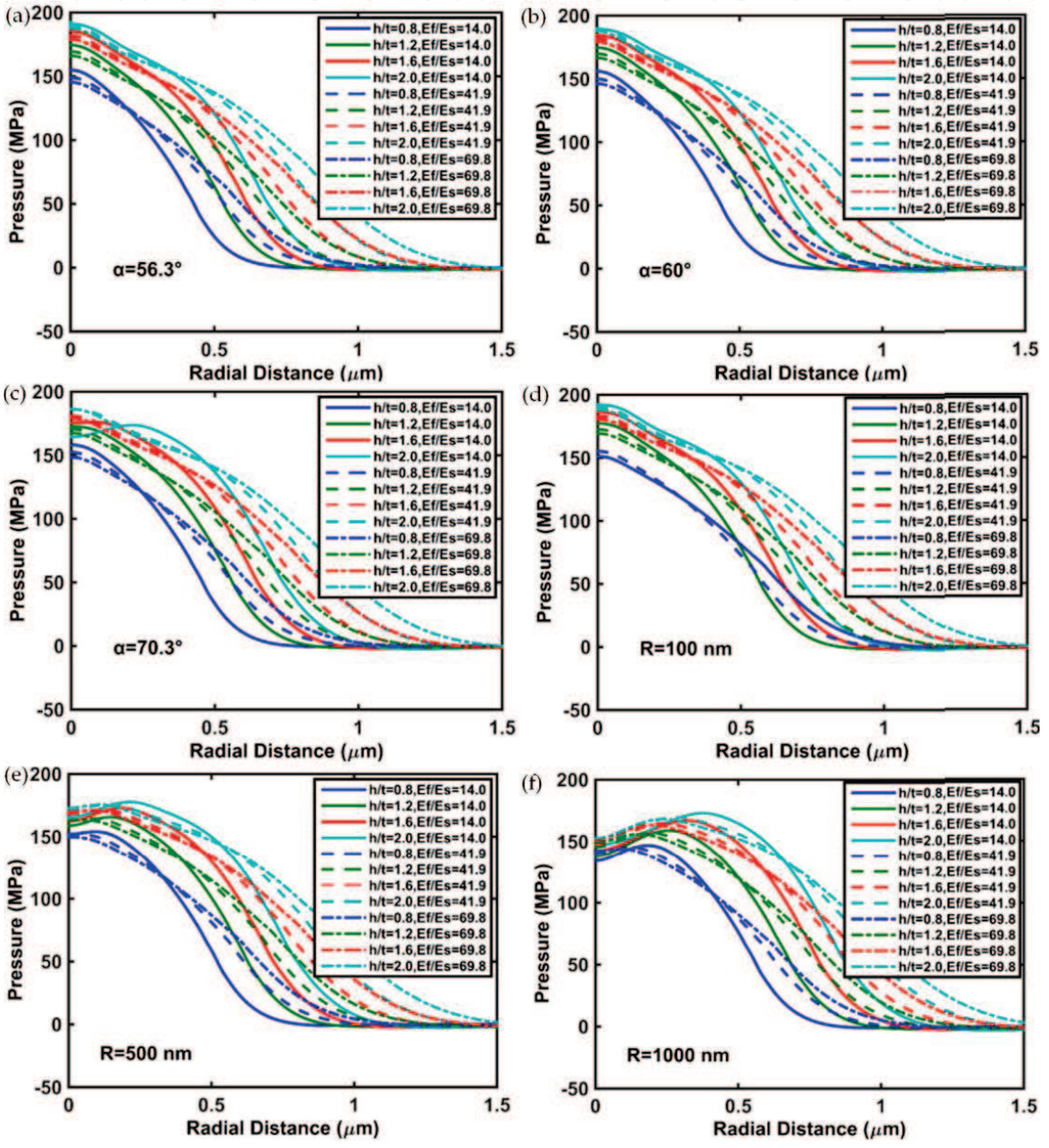

Figure 9. Pressure distribution in the interface under a conical indenter with a half-included angle α of (a) 56.3°, (b) 60.0°, and (c) 70.3°, and a spherical indenter with a radius R of (d) 100 nm, (e) 500 nm, and (f) 1000 nm [15].

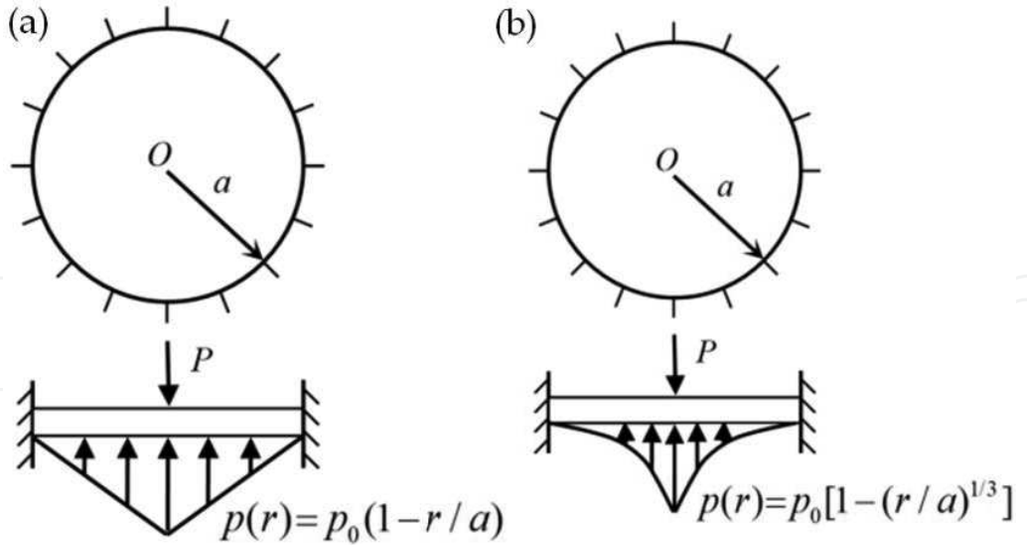

Figure 10. Schematic representation of a stress-based (a) model I and (b) model II.

In view of that, Fu et al. [15] proposed two stress-based models, as shown in **Figure 10**. The film is modeled as a circular elastic plate clamped at its edge. The radius of the circular plate, *a*, equals that of the plastic zone of the substrate beneath an axisymmetric indenter. A plastic zone of the ductile substrate beneath the film is considered as distributed pressure. Then the bending moments in films for model I and model II are given by

$$M_{\theta 1} = \frac{P}{240\pi a^3}\left(29a^3 + 29a^3\nu - 135ar^2 - 45ar^2\nu + 16r^3\nu + 64r^3\right) - \frac{P}{4\pi}\left((1-\nu)\ln\frac{a}{r} - 1\right) \tag{16}$$

$$M_{\theta 2} = \frac{P}{1456\pi a^{7/2}}\left(205a^{7/2} + 205a^{7/2}\nu - 1911a^{1/3}r^2 - 637a^{1/3}r^2\nu + 432r^{7/2}\nu + 1440r^{7/2}\right) - \frac{P}{4\pi}\left((1-\nu)\ln\frac{a}{r} - 1\right) \tag{17}$$

where *P* is the indentation load and *r* is the radial distance from the center. Subscripts 1 and 2 indicate models I and II, respectively.

The radial stress can be predicted by substituting the bending moment into Eq. (15). The normalized stresses (predicted radial stress divided by the maximum radial stress) predicted by models I and II are shown in **Figure 11**. It is clear that there is a high tensile stress outside the contact radius. Moreover, the highest compressive stress occurs at the center, which causes the radial crack. The stress obtained by the proposed models is comparable to the FE results and experimental observations [15].

After the stress distribution has been obtained, fracture toughness is obtained using linear fracture mechanics and a crack channeling criterion according to Eqs. (10)–(13) and Eq. (15).

http://dx.doi.org/10.5772/64117

It should be worth noting that the stress-based model is valid for a particular coated system only, that is, the brittle film/ductile substrate. In the next section, we introduce the mechanism of cracking in a brittle film on a ductile substrate to support the stress-based model.

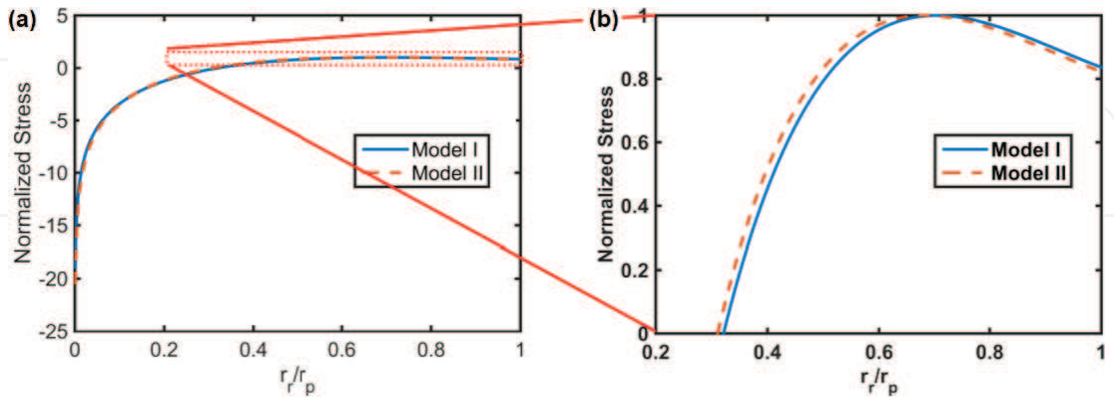

Figure 11. Normalized stress as a function of r_r/r_p (ring crack radius/plastic zone radius) predicted by the model I and model II (Poisson's ratio is assumed to be 0.21).

3. Fracture mechanism of brittle thin films under nano-indentation

Toughness measurement using a stress-based method depends strongly on the fracture mechanism of cracking. Understanding the mechanism of the crack pattern in brittle thin films could provide guidance in developing a more accurate stress-based model for toughness assessment of the film. In this section, the fracture mechanisms of various crack patterns under indentation are discussed in detail.

A number of types of crack pattern induced by an indentation in brittle thin film have been reported, such as radial cracks [16–18], ring cracks [7, 19, 20], picture-frame cracks [21, 22], spiral cracks [23, 24], and spalling [25, 26]. The crack patterns are dependent on the substrate effect, indenter shape, and the indentation load level. Regarding the substrate effect, the coated system can be divided into two types, namely the brittle film/hard substrate system and the brittle film/ductile substrate system, depending on the effects of the substrate on cracking. Accordingly, we discuss the fracture mechanisms in these two types of coated system under different types of indenter.

3.1. Crack patterns in brittle film/hard substrate

In a brittle film on a hard substrate, it has been found that cracks often occur at the contact edge of the indenter due to the stress concentration. For example, three radial cracks were detected in a diamond-like carbon (DLC) film/silicon substrate with a film thickness of 115 nm under a Berkovich indenter, as shown in **Figure 12(a)**. The radial cracks were mainly caused by the stress concentration at the contact edge. Also, a significant pileup was found around the impression. Due to the confinement of the substrate and the pileup, the radial cracks did

not propagate along the edge. Therefore, it would be invalid to use a classical method to characterize the fracture toughness of the film. For a ZnO film on an architectural glass substrate, picture-frame cracks were detected inside the impression, as shown in **Figure 12(b)**. Meanwhile, radial cracks along the indenter edge were also detected. Bull [36] argued that the picture-frame cracks were caused by the high contact stress. In addition, the FE result in **Figure 18(a)** shows that a high stress occurs around the edge of the indenter, which supports the argument of Bull [36].

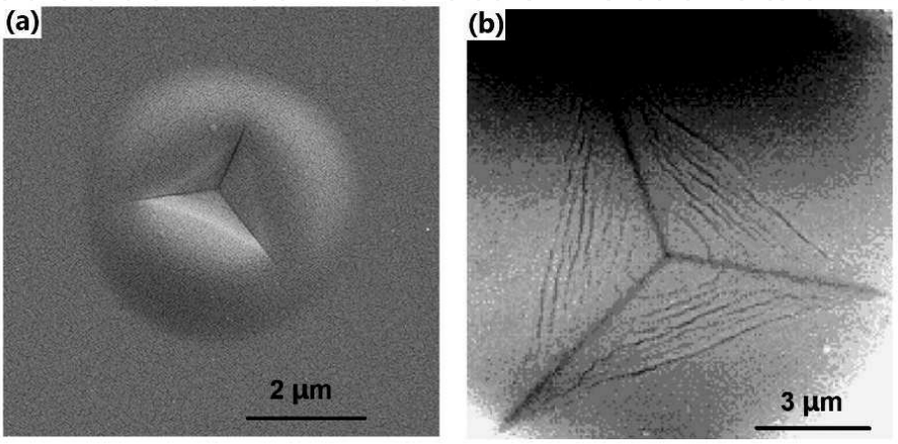

Figure 12. (a) Radial cracks and (b) picture-frame cracks [21] in a brittle film/hard substrate.

With an increase in the peak indentation load, the film on a hard substrate usually ends up with a failure of spalling, as reported in [25]. In their work, ring-like cracks together with spalling failure were observed in a DLC film caused by a conical indenter. The film outside the ring-like cracks was detached from the silicon substrate. Also, the crack pattern in a DLC film/silicon substrate caused by a cube-corner indenter was also shown in [25]. It is evident that radial cracks, ring-like cracks, and spalling occur in the films. Around the impression, the film is not detached from the substrate because of the high compressive contact stress. The spalling occurs outside the impression. It is shown that spalling occurs with a relatively higher load, regardless of the type of indenter.

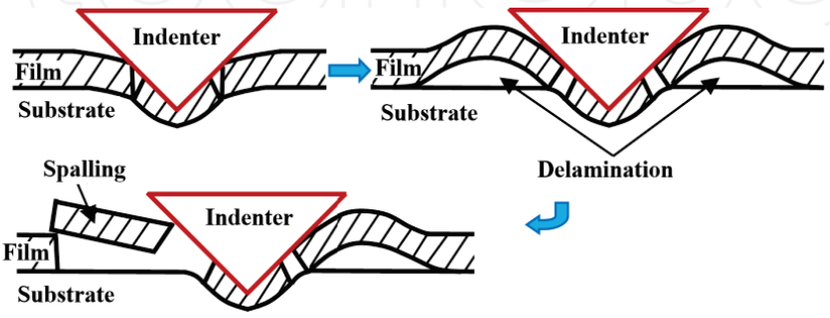

Figure 13. Schematic representation of various stages of indentation-induced cracking in a brittle film/hard substrate system.

The spalling that usually occurs in a brittle film/hard substrate follows three stages, as illustrated in **Figure 13**. First, a ring-like crack initiates and propagates toward the interface due to the high contact stress. In the second stage, delamination occurs owing to the weak bonding between film and substrate. Then the film begins to buckle because of the delamination caused by the extrusion of the indenter. In the last stage, the buckled film results in a high tensile stress. When the tensile stress reaches the film strength, the film begins to break, and spalling forms. During the formation of spalling, a significant energy release occurs, which leads to a perfect "pop-in" in the load-depth curve. Then we could measure the released energy according to the "pop-in" in the load-depth curve as described in Section 2.2.

3.2. Crack patterns in brittle film/ductile substrate

In a brittle film on a ductile substrate, the crack pattern and fracture mechanism are quite different from those in a brittle film/hard substrate system. For example, **Figure 14(a)** and **(b)** shows the crack patterns in a DLC film/polyether ether ketone (PEEK) substrate under a conical indenter and a Berkovich indenter, respectively. In **Figure 14(a)**, a few radial cracks and a ring cracks are observed. The radial cracks do not reach the ring crack, which indicates that the two types of crack are independent of each other. Examination of the stress distribution in the films in **Figure 15** shows that there is a high tensile stress on the surface of the film, and a plastic zone occurs in the substrate underneath the indenter. In the FE analysis, we found that the position of the ring crack was between the contact radius and the plastic zone, as shown in **Figure 16**. The stiffness difference between plastic zones caused the film to bend. As a result, a high tensile radial stress, which caused the ring crack formation, occurred on the surface of the indenter. It should be noted that the radial tensile stress consisted mainly of a bending stress, as well as a stretching stress in the thin film due to the contact load. If the modulus ratio of film and substrate, E_f/E_s, was significantly high, the stretching stress was negligible. In other words, the ring crack was caused mainly by film bending, which made the position of the ring crack move toward the plastic zone side. On the other hand, if E_f/E_s was low, the ring crack ran to the indenter edge. These conclusions confirmed the feasibility of the present stress-based model in Section 2.

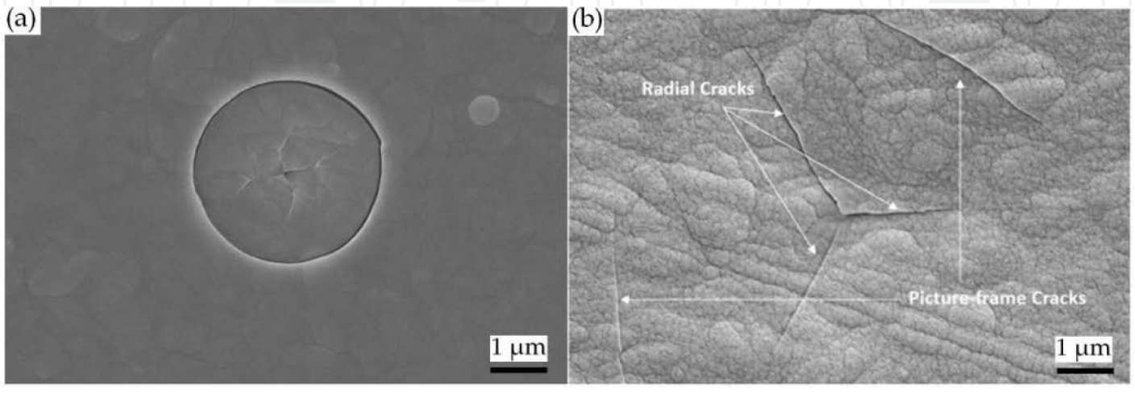

Figure 14. (a) Ring crack and (b) picture-frame crack [22] in a DLC film/PEEK substrate.

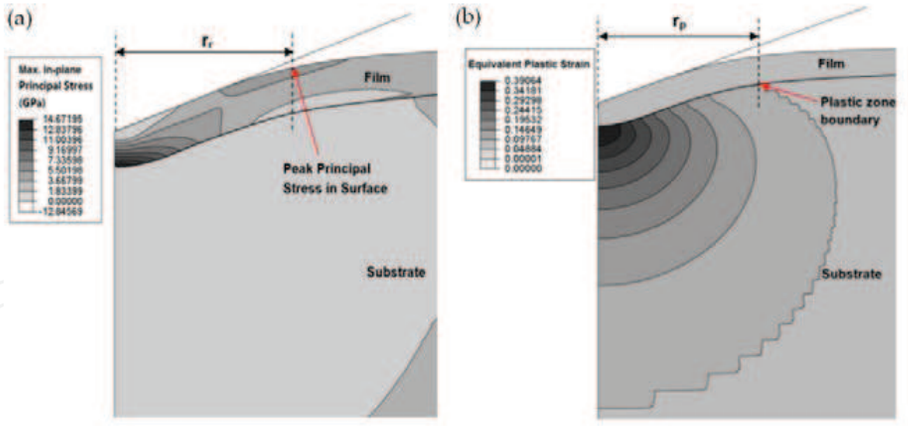

Figure 15. FE results of (a) maximum in-plane principal stress and (b) equivalent plastic strain distribution [7].

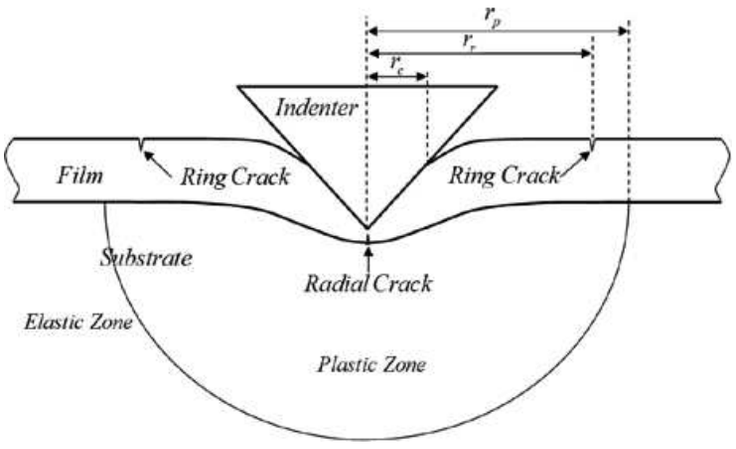

Figure 16. Fracture mechanism of a brittle film on a ductile substrate by indentation [15].

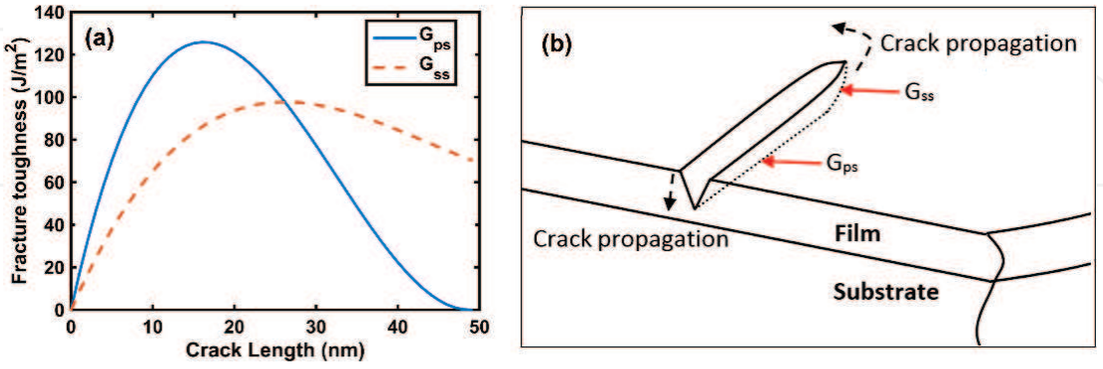

Figure 17. (a) Energy release rate of the plane strain crack G_{ps} propagating through the film and energy release rate of the channel front G_{ss} for indentation depth, and (b) illustration of a channel crack propagating through the film.

The FE analysis gives the stress distribution of film under an axisymmetric indenter, which can provide information about crack initiation. To fully understand the formation process of

http://dx.doi.org/10.5772/64117

a ring crack, more detail is necessary. Prior to the indentation, it is highly improbable that a circular defect exists in the film. The crack channeling criterion may be the best explanation for the formation of a ring crack. **Figure 17(a)** shows the energy release rate by a linear fracture mechanics and a crack channeling energy release rate. In the first stage, a pre-existing short crack exists as shown in **Figure 17(b)**. As the stress in the film increases, the crack begins to propagate toward the interface when the energy release rate by linear fracture mechanics reaches the fracture toughness. With the increase in crack length, the energy release rate by the linear fracture mechanics decreases. When it reaches the critical energy release rate for a channeling crack, the channeling ring crack initiates. The short crack adjusts its own curvature to form a ring crack because the G_{ps} at each point around the circle is the same. After that, the ring crack propagates and stops at the interface. Hence, we could obtain the fracture toughness of the brittle film on a ductile substrate if a ring crack is observed using Eq. (13).

In **Figure 14(b)**, three radial cracks were detected and two picture-frame cracks were observed outside the contact region. Also, no delamination occurred. The FE results in **Figure 18** show that the radial crack is induced by the high compressive stress due to the contact stress, which is the same as the observation in a brittle film/hard substrate. However, a high tensile stress occurs outside the contact region. With an increase in E_f/E_s, the high stress in a film surface moves outward to the contact area. The film bending by a Berkovich indenter is also controlled by the plastic zone below. After the critical stress is reached, the crack may propagate to the interface or parallel to the edge of the indenter, depending on the value of the energy release rate using the channeling crack criterion or linear fracture mechanics.

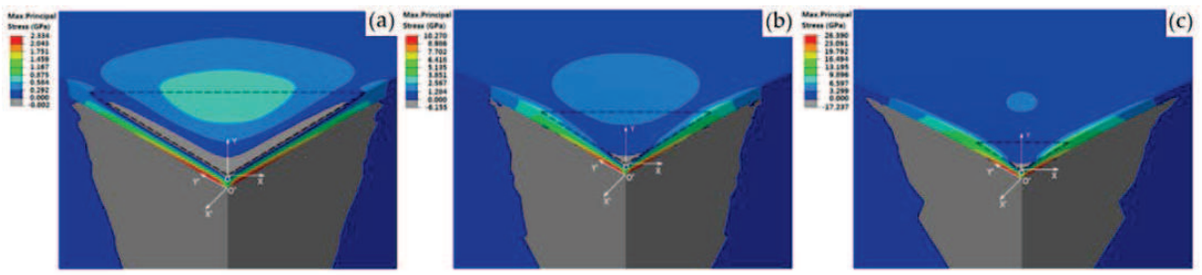

Figure 18. Maximum principal stress distribution in a brittle film on a ductile substrate (dashed lines indicate projected contact edges) with a modulus ratio of (a) $E_f/E_s = 2.3$, (b) $E_f/E_s = 14.0$, and (c) $E_f/E_s = 41.9$ [22].

If we keep increasing the indentation load in a brittle film/ductile substrate system, multiple ring cracks sometimes appear on the surface. **Figure 19** shows multiple ring cracks in a DLC film/PEEK substrate. The film thickness is 140, 400, and 1300 nm, respectively in **Figure 19(a–c)**. The peak indentation load is 10 mN. It is evident that, in all the films, there are a few radial cracks in the middle and a few ring cracks outside the radial crack. When the thickness increases to 400 nm, we can also observe a similar radial crack and ring crack pattern. In a brittle film with a high thickness, however, the crack pattern changes to a combination of both ring crack and spalling in **Figure 19(c)**. In other words, ratio of indentation depth and film thickness also affects the crack patterns. In a thin film, the ring crack is controlled by the plastic zone in the substrate under the indenter. The contribution of the plastic zone is less when a

thick film is tested because the critical depth is much smaller than the film thickness. The substrate effect might not be dominant in crack formation, and the fracture mechanism is similar to that in the bulk brittle material.

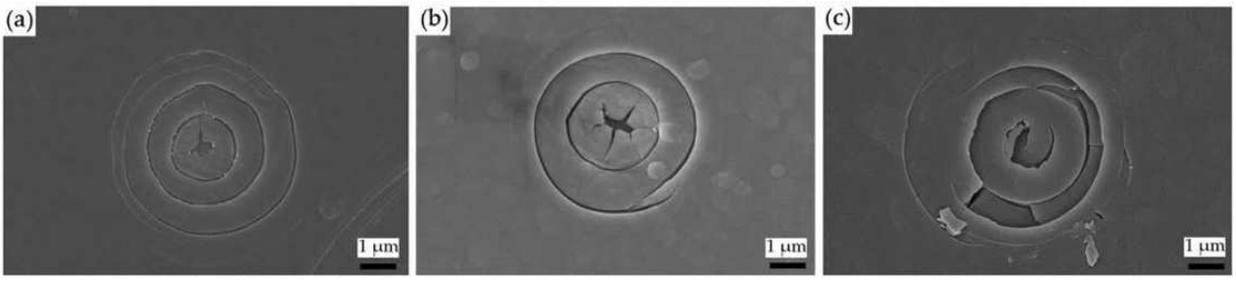

Figure 19. Multiple ring cracks in a DLC film/PEEK substrate with film thickness of (a) 140 nm, (b) 400 nm, and (c) 1300 nm.

Given the mechanism of ring crack formation, FE analysis integrated with cohesive elements can be used to simulate the formation of a ring crack. We ignore the channel crack formation here. The simulation steps are as follows:

Step 1. An FE analysis is performed without using cohesive elements. When the tensile stress in a surface reaches the tensile strength, the analysis stops, and the position of the peak tensile stress is recorded.

Step 2. Cohesive elements are inserted into the FE model at the recorded position along the thickness.

Step 3. The FE analysis is rerun, and when the tensile stress in the film surface equals the strength, a ring crack (represented by the cohesive elements) begins to initiate and propagates toward the interface. When the stress outside the first ring crack reaches the tensile strength, the position of the peak tensile stress is recorded again.

Step 4. Repeat Step 2 to insert another group of cohesive elements for the second ring crack formation.

It is seen that the FE results agree well with the experimental observations in **Figure 20**. However, it is noted that the drawback of this FE model is that it cannot simulate the propagation of a channeling crack.

Another specimen is a 100 nm Al_2O_3 film on a PEEK substrate. After indentation, there was still a multiple ring crack pattern under a conical indenter as shown in **Figure 21(a)**. We recorded the critical load and the ring crack diameter. We found the linear relation between the critical load and the diameter of the ring crack shown in **Figure 22**. In a bi-layer film, a much more complex crack pattern, a flower-shaped crack, was induced. For instance, we found that the crack pattern became a flower-shaped crack in the surface of a TiO_2/Al_2O_3 film/PEEK substrate system, as illustrated in **Figure 21(b)**. That crack is induced by the combination of

http://dx.doi.org/10.5772/64117

substrate effect and the interaction of the two brittle films. For instance, the confinement of TiO_2 film causes uncertainty of channeling crack formation.

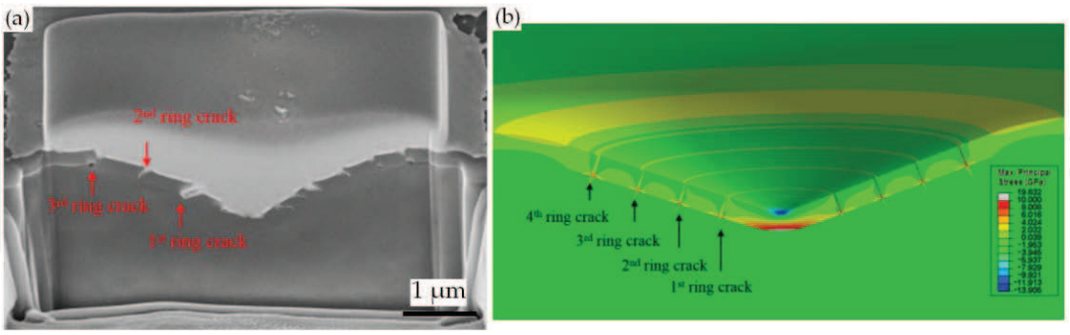

Figure 20. Focused ion beam observation of multiple ring crack and (b) simulation results of maximum principal stress, modified from [37].

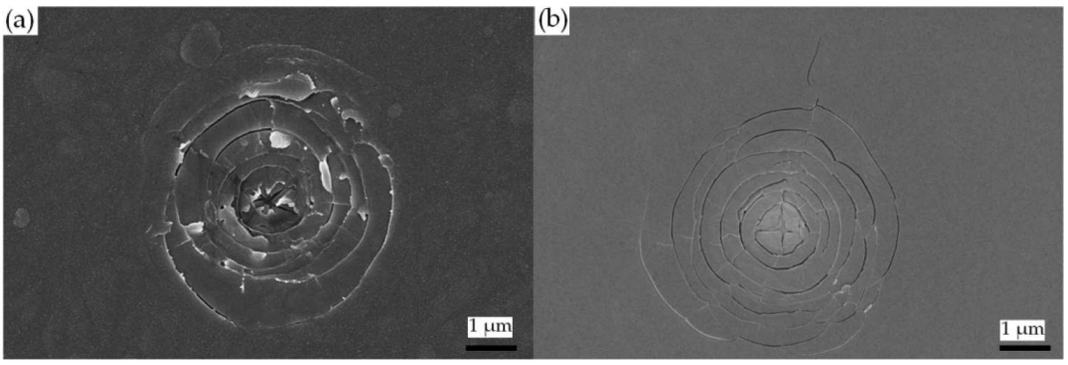

Figure 21. Crack pattern in (a) an Al_2O_3 film/PEEK substrate, and (b) a TiO_2/Al_2O_3/PEEK substrate.

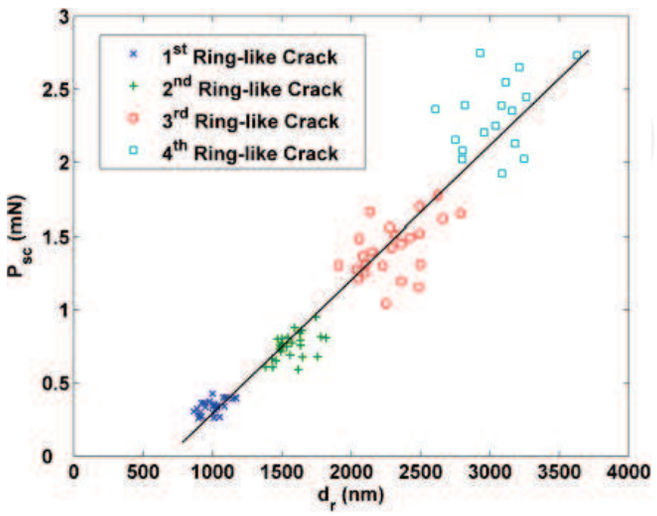

Figure 22. Critical load P_{sc} versus the diameter of ring-like crack d_r (solid lines indicate the trend) [38].

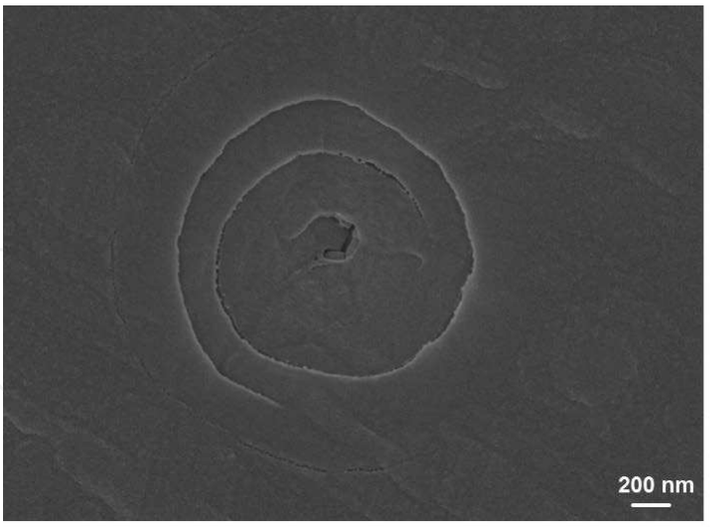

Figure 23. A spiral crack after unloading.

The spiral crack is another crack pattern induced by indentation. In **Figure 23**, a spiral crack is shown in a DLC film on a PEEK substrate. Under a conical indenter, a high equivalent stress arises near the interface owing to the film bending. Then a small defect grows to a spiral crack in the film. Once the indenter begins to withdraw, the increasing equi-biaxial stress field provides the driving force for a spiral crack extension due to the film bending curvature effect as reported in [23].

4. Summary

In this chapter, several methods for the measurement of fracture toughness of brittle film/substrate systems were presented and detailed. Fracture mechanisms for some particular crack patterns were introduced to give a better understanding of the stress-based model. The conclusions are as follows:

The classic method was a widely used method for toughness measurement in "thick" films where a radial crack was well developed. The energy method was an efficient method for determining the toughness of thin films and depends on obtaining the dissipated energy during cracking. The stress method was a straightforward method based on stress distribution and the fracture mechanism in brittle films under indentation. In particular, the fracture mechanism in brittle films depends on the substrate effect, indenter shape, and load level, which can result in different crack patterns. The FE method may be the most efficient tool to characterize the evolution of stress under indentation.

To date, there is still no generally accepted method for the measurement of brittle thin films using nano-indentation. Each method mentioned above has its limitations. In future, with a better understanding of each crack pattern, it is expected that a general stress-based solution for the toughness measurement of thin film will be developed.

http://dx.doi.org/10.5772/64117

In the meantime, a more detailed numerical model is needed to investigate the complex experimental observation. An example might be an FE model that can simulate the indentation process considering the combination of a channeling crack and delamination.

Acknowledgements

Youhong Tang is grateful for the research support of the Premier's Research and Industry Fund (PRIF) with a Catalyst Research Grant (Grant No.: CRG 65) for the research work. Li Chang is grateful for the funding from the Faculty of Engineering and Information Technologies, the University of Sydney, under the Faculty Research Cluster Program. The authors greatly acknowledge Ahmadzada for the samples of Al_2O_3 film/PEEK substrate and TiO_2/Al_2O_3/PEEK substrate.

Author details

Kunkun Fu[1], Youhong Tang[2*] and Li Chang[1]

*Address all correspondence to: youhong.tang@flinders.edu.au

1 School of Aerospace, Mechanical and Mechatronic Engineering, University of Sydney, NSW, Australia

2 School of Computer Science, Engineering and Mathematics, Flinders University, SA, Australia

References

[1] Anstis G, Chantikul P, Lawn BR, Marshall D. A critical evaluation of indentation techniques for measuring fracture toughness: I, direct crack measurements. Journal of the American Ceramic Society. 1981;64(9):533–8. DOI: 10.1111/j.1151-2916.1981.tb10321.x

[2] Ucisik AH, Bindal C. Fracture toughness of boride formed on low-alloy steels. Surface and Coatings Technology. 1997;94(5):561–5. DOI: 10.1016/s0257-8972(97)00466-0

[3] Feng W, Yan D, He J, Zhang G, Chen G, Gu W, Yang S. Microhardness and toughness of the TiN coating prepared by reactive plasma spraying. Applied Surface Science. 2005;243(1–4):204–13. DOI: 10.1016/j.apsusc.2004.09.064

[4] Cantera EL, Mellor B. Fracture toughness and crack morphologies in eroded WC–Co–Cr thermally sprayed coatings. Materials Letters. 1998;37(4–5):201–10. DOI: 10.1016/s0167-577x(98)00092-5

[5] Xie X, Guo H, Gong S, Xu H. Lanthanum–titanium–aluminum oxide: a novel thermal barrier coating material for applications at 1300 °C. Journal of the European Ceramic Society. 2011;31(9):1677–83. DOI: 10.1016/j.jeurceramsoc.2011.03.036

[6] Li XD, Diao DF, Bhushan B. Fracture mechanisms of thin amorphous carbon films in nanoindentation. Acta Materialia. 1997;45(11):4453–61. DOI: 10.1016/s1359-6454(97)00143-2

[7] Fu KK, Yin YB, Chang L, Shou DH, Zheng BL, Ye L. Analysis on multiple ring-like cracks in thin amorphous carbon film on soft substrate under nanoindentation. Journal of Physics D: Applied Physics. 2013;46: 505314. DOI: 10.1088/0022-3727/46/50/505314

[8] Chen J, Bull SJ. Assessment of the toughness of thin coatings using nanoindentation under displacement control. Thin Solid Films. 2006;494(1–2):1–7. DOI: 10.1016/j.tsf.2005.08.176

[9] den Toonder J, Malzbender J, de With G, Balkenende R. Fracture toughness and adhesion energy of sol-gel coatings on glass. Journal of Materials Research. 2002;17(1):224–33. DOI: 10.1557/jmr.2002.0032

[10] Chen J, Bull SJ. Modelling the limits of coating toughness in brittle coated systems. Thin Solid Films. 2009;517(9):2945–52. DOI: 10.1016/j.tsf.2008.12.054

[11] Steffensen S, Madsen ND, Jensen HM. Numerical estimation of fracture toughness from indentation-induced circumferential cracking in thin films on ductile substrates. International Journal of Solids and Structures. 2013;50(20–21):3406–17. DOI: 10.1016/j.ijsolstr.2013.06.009

[12] Madsen ND, Steffensen S, Jensen HM, Bøttiger J. Toughness measurement of thin films based on circumferential cracks induced at conical indentation. International Journal of Fracture. 2015;193(2):117–30. DOI: 10.1007/s10704-015-0022-5

[13] Steffensen S, Jensen HM. Energy release rate for circular crack due to indentation in a brittle film on a ductile substrate. European Journal of Mechanics-A/Solids. 2014;43:133–41. DOI: 10.1016/j.euromechsol.2013.09.010

[14] Morasch KR, Bahr DF. Nanomechanical testing for fracture of oxide films. Journal of Materials Research. 2005;20(06):1490–7. DOI: 10.1557/jmr.2005.0188

[15] Fu KK, Chang L, Ye L, Yin YB. Indentation stress-based models to predict fracture properties of brittle thin film on a ductile substrate. Surface and Coatings Technology. 2016;296:46-57. DOI: 10.1016/j.surfcoat.2016.03.067

[16] Volinsky AA, Vella JB, Gerberich WW. Fracture toughness, adhesion and mechanical properties of low-K dielectric thin films measured by nanoindentation. Thin Solid Films. 2003;429(1–2):201–10. DOI: 10.1016/s0040-6090(03)00406-1

[17] Karimi A, Wang Y, Cselle T, Morstein M. Fracture mechanisms in nanoscale layered hard thin films. Thin Solid Films. 2002;420:275–80. DOI: 10.1016/s0040-6090(02)00944-6

[18] Zhang S, Zhang X. Toughness evaluation of hard coatings and thin films. Thin Solid Films. 2012;520(7):2375–89. DOI: 10.1016/j.tsf.2011.09.036

[19] Hainsworth SV, McGurk MR, Page TF. The effect of coating cracking on the indentation response of thin hard-coated systems. Surface and Coatings Technology. 1998;102(1–2): 97–107. DOI: 10.1016/s0257-8972(97)00683-x

[20] Thomsen NB, Fischer-Cripps AC, Swain MV. Crack formation mechanisms during micro and macro indentation of diamond-like carbon coatings on elastic–plastic substrates. Thin Solid Films. 1998;332(1–2):180–4. DOI: 10.1016/s0040-6090(98)01101-8

[21] Chen J, Bull SJ. Indentation fracture and toughness assessment for thin optical coatings on glass. Journal of Physics D: Applied Physics. 2007;40(18):5401. DOI: 10.1088/0022-3727/40/18/s01

[22] Fu KK, Chang L, Zheng BL, Tang YH, Yin YB. Analysis on cracking in hard thin films on a soft substrate under Berkovich indentation. Vacuum. 2015;112:29–32. DOI: 10.1016/j.vacuum.2014.11.013

[23] Yonezu A, Liu L, Chen X. Analysis on spiral crack in thick diamond-like carbon film subjected to spherical contact loading. Materials Science and Engineering: A. 2008;496(1):67–76. DOI: 10.1016/j.msea.2008.04.069

[24] Xie ZH, Munroe PR, McGrouther D, Singh RK, Hoffman M, Bendavid A, Martin PJ, Yew S. Three-dimensional study of indentation-induced cracks in an amorphous carbon coating on a steel substrate. Journal of Materials Research. 2006;21(10):2600–5. DOI: 10.1557/jmr.2006.0313

[25] Li X, Bhushan B. Measurement of fracture toughness of ultra-thin amorphous carbon films. Thin Solid Films. 1998;315(1–2):214–21. DOI: 10.1016/s0040-6090(97)00788-8

[26] Evans AG, Hutchinson JW. On the mechanics of delamination and spalling in compressed films. International Journal of Solids and Structures. 1984;20(5):455–66. DOI: 10.1016/0020-7683(84)90012-x

[27] Lawn BR, Evans A, Marshall D. Elastic/plastic indentation damage in ceramics: the median/radial crack system. Journal of the American Ceramic Society. 1980;63:574–81. DOI: 10.1111/j.1151-2916.1980.tb10768.x

[28] Strecker K, Ribeiro S, Hoffmann MJ. Fracture toughness measurements of LPS-SiC: a comparison of the indentation technique and the SEVNB method. Materials Research. 2005;8:121–4. DOI: 10.1590/s1516-14392005000200004

[29] Dukino RD, Swain MV. Comparative measurement of indentation fracture toughness with Berkovich and Vickers indenters. Journal of the American Ceramic Society. 1992;75:3299–304. DOI: 10.1111/j.1151-2916.1992.tb04425.x

[30] Pharr G. Measurement of mechanical properties by ultra-low load indentation. Materials Science and Engineering: A. 1998;253(1–2):151–9. DOI: 10.1016/s0921-5093(98)00724-2

[31] Marshall D, Lawn B. An indentation technique for measuring stresses in tempered glass surfaces. Journal of the American Ceramic Society. 1977;60:86–7. DOI: 10.1111/j.1151-2916.1977.tb16106.x

[32] Yang F. Axisymmetric indentation of an incompressible elastic thin film. Journal of Physics D: Applied Physics. 2003;36(1):50. DOI: 10.1088/0022-3727/36/1/307

[33] Yang F. Asymptotic solution to axisymmetric indentation of a compressible elastic thin film. Thin Solid Films. 2006;515(4):2274–83. DOI: 10.1016/j.tsf.2006.07.151

[34] Sburlati R. Elastic indentation problems in thin films on substrate systems. Journal of Mechanics of Materials and Structures. 2006;1(3):541–57. DOI: 10.2140/jomms.2006.1.541

[35] Sburlati R. Adhesive elastic contact between a symmetric indenter and an elastic film. International Journal of Solids and Structures. 2009;46(5):975–88. DOI: 10.1016/j.ijsolstr.2008.10.006

[36] Bull SJ. Analysis methods and size effects in the indentation fracture toughness assessment of very thin oxide coatings on glass. Comptes Rendus Mecanique. 2011;339(7–8):518–31. DOI: 10.1016/j.crme.2011.05.009

[37] Fu KK, Zheng BL, Yin YB, Hu TY, Ye L, Shou DH. Fracture analysis of diamond-like carbon films under conical nanoindentation. Journal of University of Science and Technology Beijing. 2014;36:70–6. DOI: 10.13374/j.issn1001-053x.2014.02.011

[38] Fu KK, Chang Y, Chang L, Zheng BL. An improved indentation method for estimating limits of fracture toughness in brittle films. Advanced Materials Research. 2015;1095:598–602. DOI: 10.4028/www.scientific.net/amr.1095.598